energies

MDPI

Article

South Anze Structure and Its Control on Coalbed Methane Aggregation in the Qinshui Basin and the Mechanism of Syncline Gas Enrichment in the Qinshui Basin

Bo Wang [1], Qingtian Zhang [2,3], Zhenghui Qu [2,3,*] and Yiteng Zhang [1]

1 Information Institute of the Ministry of Emergency Management of PRC, Beijing 100029, China
2 Key Laboratory of Coalbed Methane Resources and Reservoir Formation Process of the Ministry of Education, China University of Mining and Technology, Xuzhou 221116, China
3 School of Resources and Geosciences, China University of Mining and Technology, Xuzhou 221116, China
* Correspondence: quzhenghui@cumt.edu.cn

Abstract: The phenomenon of coalbed-methane synclinal accumulation in the Qinshui Basin has been widely reported, but it has mainly been observed in the core block of the Qinshui Syncline. The questions arise: does this phenomenon exist in the wing of the Qinshui Syncline and, if so, what is the mechanism behind it? Further study is required to answer these questions. This paper focuses on the South Anze No. 3 coal seam in the Qinshui Basin as an example. It conducts a systematic sorting of coalbed-methane geological characteristics and an analysis of the effects of structural assemblage characteristics, genetic mechanisms, and structural control on coalbed-methane accumulation. Additionally, it examines the basin structure and evolution during the critical period of the Qinshui Basin, as well as the gas geological characteristics of adjacent areas, in order to discuss the gas-rich mechanism of the syncline in the Qinshui Basin. Key insights obtained from the study include the following: (i) The whole South Anze is a nosing structure that plunges from west to east and superposes secondary folds and faults in different directions. Four deformation zones can be identified based on the characteristics of structural assemblage, including NEN-oriented compressive structures, ENE-trend shear fractures, EW-trend compressive fractures, and EW-trend compressive folds. The formation of structural assemblage in the study area is attributed to the compression in the Indosinian and Yanshanian, and the fault inversion in the Himalayan period. (ii) The ENE-trend shear fracture deformation area located in the nosing uplift is a low CBM (coalbed methane) content area due to gas diffusion during the Himalayan extension. The syncline in the combination of NEN-trend and EW-trend "ejective folds" in the west and south of the study area is a high-value area of coalbed-methane content. It is further verified that the law of syncline gas accumulation in the Qinshui Basin is also applicable to the wing of the Qinshui Syncline. (iii) Since the formation of the Qinshui Syncline, the main coal seam has been in an extensional environment below the neutral plane, resulting in the main dissipation of coalbed methane. During its geological history, surface water penetrated the aquifer above the main coal seam through two channels: the extensional area above the neutral plane of the adjacent anticline and the shear fracture. A hydrostatic pressure seal is formed in the Qinshui Syncline and the secondary syncline is superimposed upon it, which is the cause of gas enrichment in the syncline of the Qinshui Basin. (iv) Weak deformation in the syncline basin is the focus of global coalbed-methane exploration and development. The mechanism proposed in this paper can provide ideas and references for further understanding of coalbed-methane enrichment in this type of basin.

Keywords: South Anze; tectonic deformation; coalbed methane aggregation; "ejective fold"; gas synclinal accumulation

check for updates

Citation: Wang, B.; Zhang, Q.; Qu, Z.; Zhang, Y. South Anze Structure and Its Control on Coalbed Methane Aggregation in the Qinshui Basin and the Mechanism of Syncline Gas Enrichment in the Qinshui Basin. *Energies* **2023**, *16*, 4521. https://doi.org/10.3390/en16114521

Academic Editor: Krzysztof Skrzypkowski

Received: 28 February 2023
Revised: 17 May 2023
Accepted: 18 May 2023
Published: 4 June 2023

1. Introduction

The importance of structure in coalbed-methane enrichment is widely accepted by geologists. It has a significant impact on the storage characteristics of coalbed methane [1].

Together with hydrodynamic conditions, structure constitutes two important geological factors for coalbed-methane enrichment [2,3]. Qin et al. (2008) [4] emphasize the role of tectonics in controlling coalbed-methane accumulation. They believe that coalbed-methane accumulation is controlled by many macro-geological dynamic conditions, including tectonic dynamics, thermal dynamics, and groundwater dynamics. The tectonic dynamic conditions balance other dynamic conditions and are the fundamental factors controlling the accumulation effect of coalbed methane. The coalbed-methane accumulation effect of the structure is divided into three levels: basin, basin structure, and coal reservoir. This study focuses on the structural level in the basin, specifically the influence of different structural styles and their controlled preservation conditions on coalbed-methane enrichment.

There have been many previous research results on the enrichment effect of coalbed methane in structural styles, mainly involving the impact of different types of structures in structural development areas and their combination with hydrodynamic conditions on coalbed-methane enrichment. Scholars have a relatively unified understanding of the fault effect, believing that compressive faults form closed fault planes, which are conducive to the enrichment of coalbed methane, while tensile faults are prone to unfavorable enrichment due to the development of tensile fractures in coal seams and surrounding rocks [5–8]; Liu et al. (2022) [9,10] further limited the effective distance of faulting effects on coalbed-methane content to within 1000 m based on research in the Qinshui Basin. In contrast, the understanding of the folding effect is a gradually deepening and improving process, and the performances of anticline and syncline are different. The axis of anticline is often not favored due to the shallow burial depth of folding uplift and often being in the hydrodynamic runoff zone, while syncline is relatively deeply buried in depressions and influenced by the centripetal mechanism of formation water: it is a recognized location for coalbed-methane enrichment [5–7,11,12]. However, further research combining the effects of a fold neutral plane and gas critical depth indicates that the strength of the sealing ability caused by stress or the thickness of the cover layer is also a key factor in determining the gas control of the anticline: if strong, gas formed from the two wings gathers to the axis of the anticline to form a "gas cap"; if weak, it forms an "escape window" and a low gas content unit. However, if it communicates with the atmosphere or surface water to form hydraulic sealing, it can assist in the formation of coalbed-methane reservoirs on both wings [13–17]. As for the syncline, if the coal seam is located below the neutral plane, the axial coal seam becomes an unfavorable location for coalbed-methane enrichment due to thickness reduction and crack development. Favorable gas reservoirs can be formed only when there are compressive faults or hydraulic sealing on the two wings [15].

The above studies mainly focus on tectonically developed areas, and the coalbed-methane enrichment effect of weak deformation in tectonically simple development areas is not much discussed while, in fact, successful coalbed-methane development blocks across the world are mostly located in weakly deformed and tectonically simple basins. For example, the American San Juan, Australian Surat, and Chinese Qinshui basins are all gently dipping large synclines with a series of weakly deformed secondary folds [18–23], and these weakly deformed folds at different scales have an obvious controlling effect on coalbed-methane enrichment [16,24,25]. However, there are few research results on the mechanism of coalbed-methane formation in weakly deformed structures, and the following is an example to summarize them in the Qinshui Basin.

The Qinshui Basin is a relatively weakly deformed basin developed in the craton [26,27]. It is a pioneer in the exploration and development of coalbed methane in China. A discussion on the enrichment of coalbed methane related to its structure can serve as good material for summarizing the coalbed-methane enrichment effect of weak deformation. It can be generally divided into three aspects. Firstly, it is related to fault, and the understanding is consistent with the strong structural deformation area. The coalbed-methane content in the area with a developed tensile fault is low, while that in the area with a developed compressive fault is the opposite [9,28,29]. Secondly, coalbed-methane content is related to fold, and its understanding is relatively simple compared to the "strong deformation area", which means that the gas content in the syncline is high and in the anticline is low [9,10,30,31]. Thirdly, coalbed-methane content is related to structure and water. It is considered that the hydrodynamic retention area under the control of structure, including the footwall of the fault and the hinge of the syncline, is the coalbed-methane enrichment area [7,30–32]. In comparison with the strong deformation area, water plays a role in plugging in different ways. The sealing water in the weak deformation zone comes from the retention of the overlying aquifer and is controlled by hydrostatic pressure. The water in the plugging effect of the latter comes from the injection of the recharge area, which belongs to the control of hydrodynamic pressure. Therefore, it is not difficult to determine the law of coalbed-methane enrichment in the Qinshui Basin. The water detained in the structural origin low point seals coalbed methane to realize enrichment. A recent study by Liu et al. [10] represents the latest knowledge. The coal reservoir in the Qinshui Basin is mostly of low permeability and coalbed-methane unsaturated, meaning there is no capacity for long-distance upward migration as a conventional natural gas. At the same time, the coal reservoir is saturated with water, and the coalbed methane is controlled in the syncline or the low point of the structure by hydrostatic pressure. However, there are still some aspects to be improved as follows:

Firstly, the law of the syncline controlling gas is mostly found in the core block of the Qinshui Syncline, and whether it is applicable to the wing needs to be verified. Secondly, details are incompletely considered in the description of various geological processes in the genetic interpretation. The South Anze area is located in the west wing of the Qinshui Syncline, superimposing weak fold deformation and fault structure in different directions, with a large change in coalbed-methane content, which is a favorable area for verification of a new area. Thirdly, the vertical and horizontal ratios of structural sections are inconsistent, which cannot truly reflect the deformation characteristics of the basin. In this study, the No. 3 coal seam is taken as the research object and, on the basis of a systematical summarization of the geological conditions of coalbed methane, an analysis is carried out regarding the tectonic deformation field, deformation sequence, and assemblage characteristics by restoring the real deformation characteristics of the study area. This work then further explores the tectonic gas-controlling effect, focuses on the water and gas transport and gathering process during the critical period of tectonics in the Qinshui Basin, and discusses the mechanism of gas enrichment.

2. Geological Background

The study area, located in the North China craton, is at the intersection of three tectonic domains: paleo-Asian ocean, Tethys ocean, and marginal-Pacific. During the early Paleozoic era, a continental sea environment prevailed, and a series of marine strata, dominated by carbonate, were deposited. The late Caledonian movement caused a whole-plate uplift, interrupting the deposition and accepting erosion, resulting in a parallel unconformity between the early and late Paleozoic strata. Starting from the late Carboniferous, the plate sank and received sedimentation as a whole, continuing until the late Triassic, forming a set of sedimentary strata that gradually evolved from marine to terrestrial, including two sets of coal-bearing formations, the late Carboniferous–early Permian Taiyuan formation and the Shanxi formation. Since the formation of the late Paleozoic coal-bearing strata, they have been successively subjected to SN-trending tectonic stress in the Hercynian paleo-Asian ocean tectonic domain and Indosinian Tethys ocean tectonic domain, WNW–ESE-trending tectonic stress in the Yanshanian Pacific tectonic domain, and extensional tectonic stress under the combined effect of NEN–SWS-trending compression in the neo-Tethys ocean tectonic domain and backward movement of the Pacific plate subduction in the Himalayan (Figure 1a). This process formed two stable and continuous structural layers of Є-O and C-T in the Qinshui Basin, separated by three parallel unconformity interfaces (Table 1). Simultaneously, the corresponding structural features of coal measures were created.

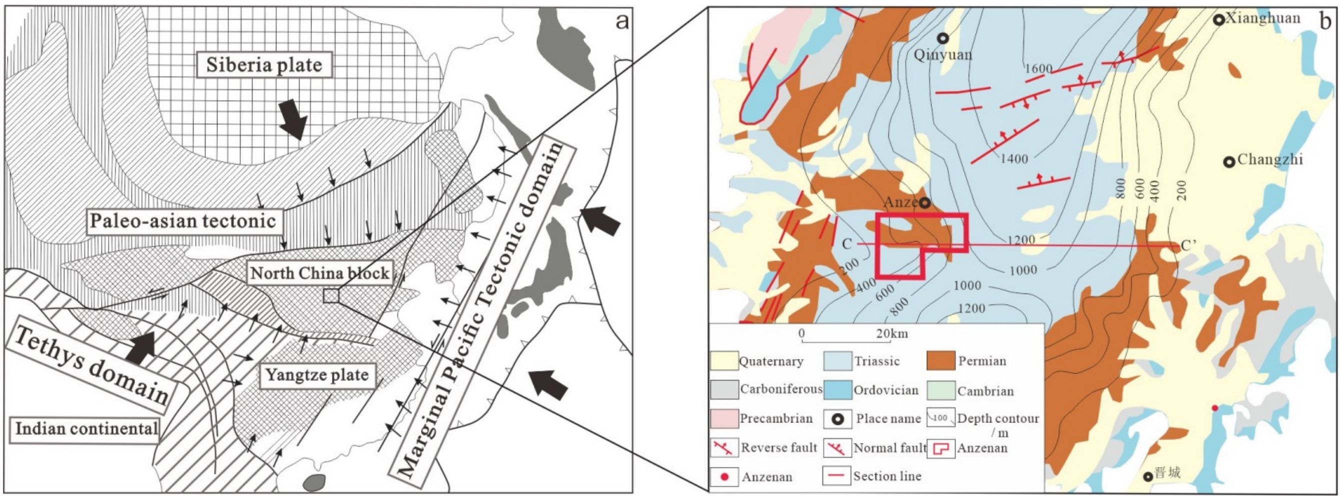

Figure 1. Geotectonic location and geological map of the southern Qinshui Basin [3,33]. (**a**) The tectonic location of the southern Qinshui Basin. (**b**) Geological map of the southern Qinshui Basin and tectonic location of the study area.

The southern Qinshui Basin, situated in the south of the central part of the North China plate, is an example of the above. The outcrop characteristics of the strata and the structural features reflected by the contour line of the buried depth of the lower Shihezi formation (Figure 1b) show that the stratum outcrop line and the buried depth contour line extend in the NEN–SSW direction, surrounded by the SWS end. The Triassic is exposed in the center, and the Permian, Carboniferous, Ordovician, Cambrian, and Precambrian are successively exposed to the periphery. The buried depth of the lower Shihezi formation gradually becomes shallow from the center to the periphery, indicating that the southern Qinshui Basin is mainly controlled by a syncline structure that strikes NEN and rises to SWS, reflecting the WNW–ESE compressive stress in the region. The exposed Permian in the South Anze area bulges to the east compared with the north and south adjacent areas, and the contour map of the burial depth of the lower Shihezi formation shows the details of deformation more clearly. It is a nosing structure extending in the EW-trend and plunging eastward, indicating compression stress in the NS-oriented in the region. At the same time, to the east of the dipping end of the nosing structure, the contour map of the buried depth of the lower Shihezi formation shows a narrow and long low uplift in the EW direction, which divides the NEN Qinshui Syncline into two relatively independent units in the north and south. The low uplift and the nosing structure belong to the same near EW-trend anticline and were formed under the action of near NS-oriented compressive stress. Later, the NEN-trend Qinshui Syncline was superimposed to form a nosing structure and low uplift structure in the west wing and hinge of the Qinshui Syncline.

The tectonic deformation of South Anze is weak, and the stratigraphic inclination is mostly NE-oriented and SE-oriented. Local areas may lean towards NW due to the influence of wide and gentle folds, and the dip angle of the strata is generally 7–15°. The outcrop in the area is relatively simple, from old to new, it is the upper Permian upper Shihezi formation and Shiqianfeng formation, and the lower Triassic Liujiagou formation (Figure 2). The coal-bearing strata in the study area are mainly the Taiyuan formation and Shanxi formation. The No. 9, No. 10, and No. 11 coal seams of the Taiyuan formation and the No. 3 coal seam of the Shanxi formation are stable coal seams that can be mined throughout the area. This paper's research focuses on the No. 3 coal seam.

Table 1. Regional stratigraphic table of the Qinshui Basin [34].

Erathem	System	Series	Group or Formation	Codename	Thickness (m)	Lithology	Tectonic Period
Neozoic	Quaternary			Q	0–550	Loess, sub-clay	Himalayan
	Neogene			N	0–200	Clay, siltstone	
Mesozoic		Middle Jurassic	Heifeng Formation	J_2h	0–220	Gray green, gray yellow quartz sandstone, glutenite	Yanshanian
	Triassic	Upper Series	Yanchang Group	T_3yn	30–140	Grayish red, grayish green sandstone, shale and freshwater limestone	Indosinian
		Middle Series	Tongchuan Formation	T_2t	396–591	Light red, gray yellow feldspar sandstone with sandy mud shale	
				T_2er	467–742	Gray-green, purple-red feldspar sandstone, mudstone and shale	
		Lower Series	Heshanggou Formation	T_1h	131–474	Purple red feldspar sandstone with purple red mudstone	
			Liujiagou Formation	T_1l	115–595	Gray purple feldspar sandstone with shale and conglomerate	
			Shiqianfeng Formation	P_2sh	22–217	Yellow-green feldspar sandstone and purple mudstone interbedded	
Upper paleozoic	Permian	Upper Series	Upper Shihezi Formation	P_2s	220–2217	Grey green quartz sandstone and purple red siltstone interbedded	Hercynian
		Middle Series	Lower Shihezi Formation	P_1x	70–360	Yellow-green mudstone, siltstone and sandstone with thin coal seams at the bottom	
	Carboniferous	Lower Series	Shanxi Formation	P_1s	36–132	Gray green quartz sandstone and shale, limestone and coal seam	
			Taiyuan Formation	C_2t	82–142	Gray quartz sandstone, shale, limestone and coal seams	
		Upper Series	Benxi Formation	C_2b	0–35	Variegated aluminite, claystone and limestone, with iron ore at the bottom	
Lower Paleozoic	Ordovician	Middle Series	Fengfeng Formation	O_2f	0–176	Middle leopard limestone, dolomite and black limestone	Caledonian
			Upper majiagou Formation	O_2s	170–308	Dolomitic marl, leopard skin and brecciated limestone	
			Lower Majiagou Formation	O_2x	37–213	Thick limestone, brecciated limestone, calcareous shale at the bottom	
		Lower Series	Liangjiashan Formation	O_1l	105	Light gray thick dolomite, flint and concretion dolomite	
			Yeli Formation	O_1y	49	Lower argillaceous and bamboo-leaf dolomite	
	Cambrian	Upper Series	Fengshan Formation	$Є_3f$	38–109	Thick layered crystal, bamboo leaf and oolitic dolomite	
			Longshan Formation	$Є_3c$	6–35	Bamboo leaf limestone, dolomite and yellow green shale	
			Gushan Formation	$Є_3g$	15–42	Mud bands, bamboo leaf limestone and shale	
		Middle Series	Zhang Xia Group	$Є_2z$	65–244	Oolitic limestone, bottom thin limestone and shale interbedding	
			Xuzhuang Formation	$Є_2x$	32–169	Oolitic and strip limestone interbedded, bottom sand shale	
			Maozhuang Formation	$Є_2m$	5–92	Purple red shale is interbedded with limestone and mudstone, and the top is oolitic limestone.	
		Lower Series	Steamed bread Formation	$Є_1m$	35–86	Yellow-green shale, marl, basal pebbly sandstone	
			Xinji Formation	$Є_1x$	29–54	Dolomite with limestone, lower red quartz sandstone	
neoproterozoic	Sinian			Z-Jx	31–1268	Purple-gray-white boulders-glutinite, quartz sandstone siltstone and shale, with dolomite mudstone	

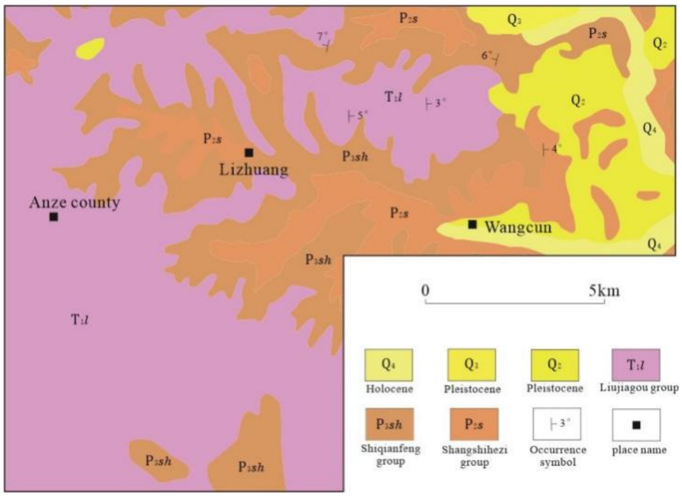

Figure 2. South Anze geological map.

3. Coalbed-Methane Geology

Based on the geological survey report of the South Anze area, this chapter systematically compares the CBM geological characteristics from three perspectives: source rock, reservoir, and preservation condition, based on the introduction of the coal seam and CBM distribution of the No. 3 coal seam.

3.1. Distribution of Coal Seam and Coalbed Methane of the No. 3 Coal Seam

(i) Buried depth and thickness of the No. 3 coal seam

The depth at which the coal seam is buried is a key factor that affects its permeability, gas content, and gas saturation. In this study area, the coal-seam depth ranges from 450 to 950 m, belonging to a medium buried depth. The area can be roughly divided into east, north, and south zones, which exhibit different changing patterns. The eastern zone is controlled by NEN-trending folds and faults, with the buried depth contour extending in the NEN orientation and fluctuating from west to east. This creates two burial centers: one is located in the west of A502, controlled by faults, with a maximum buried depth of over 900 m, which is the deepest buried area in the study area. The other center is located in A704, controlled by a syncline, with a maximum buried depth of 800 m. In the north and south zones, the depth contours are nearly EW-oriented and NE-oriented, respectively, and form two shallow burial zones in the South Anze area, with central burial depths of 600 and 550 m, respectively (Figure 3). Most coal seams in the study area are buried in the saturated adsorption zone (600–1800 m), which is favorable for coalbed-methane accumulation [16].

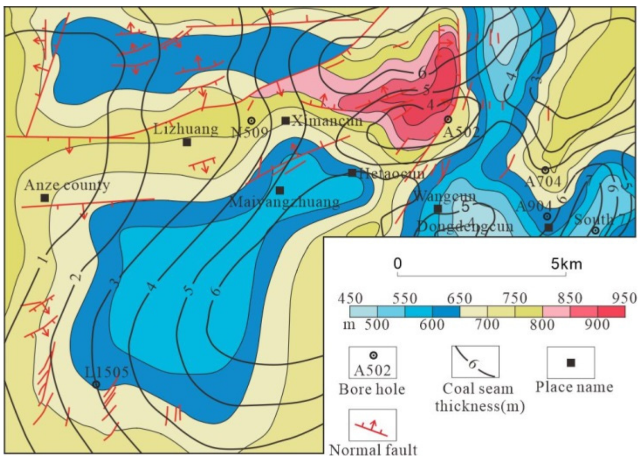

Figure 3. Isoline map of buried depth and thickness of the No. 3 coal seam in South Anze.

The thickness of the No. 3 coal seam in South Anze area varies from east to west with the Maiyangzhuang–Ximangou line as the boundary. The western area is relatively simple, with isoline extending in the NNE orientation and gradually increasing in thickness from west to east. There are significant changes in the eastern zone, with multiple thick and thin coal centers, including three thick centers. The southeast corner of the study area has the largest thickness (thickness over 7 m), but the range is small. The other two are close to the western boundary of the eastern zone, and there are two thickness centers with a thickness of over 6 m in the north and south. There are also three thin coal centers, with the one located in the northeast corner being the thinnest (less than 3 m) but having a large distribution area, and the other two located in A502 and south Wangcun, respectively, with the thinnest part of less than 4 m and a small distribution area (Figure 4). In general, the thickness of the South Anze No. 3 coal seam is mostly thick (3.5–8 m), which is favorable for coalbed-methane enrichment, and the eastern is obviously better than the western region.

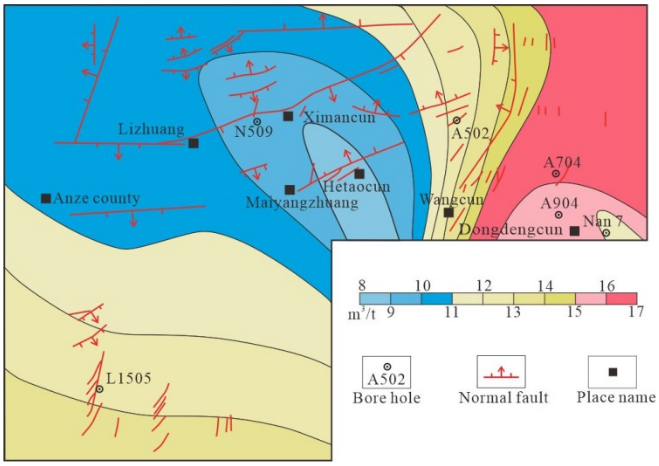

Figure 4. Contour map of coalbed-methane content in the No. 3 coal seam of South Anze.

(ii) Coalbed-methane content of the No. 3 coal seam

The content of coalbed methane in the study area is relatively high, ranging from 8 to 17 m^3/t, with great variation and significant regularity, and it gradually increases eastward and southward with the Hetaozhuang–Simangou line as the center (Figure 4). In the low-value center of Hetaozhuang–Ximangou, the isoline is in the NW orientation, with the lowest value of 8 m^3/t; in the gas content increasing areas to the east and south, the isolines are in the NEN orientation and WNW orientation, with the highest values of 17 and 15 m^3/t, respectively. In addition, a relatively low-value center is developed around Nan 7 in the southeast corner of the South Anze area, with the lowest gas content of 11 m^3/t, resulting in a peak gas content area in the north of A904.

3.2. Source Rock and Reservoir Conditions of the No. 3 Coal Seam

(i) Source rock of the No. 3 coal seam

According to the experimental data, the No. 3 coal seam in the study area is of medium and low volatility and extra-low sulfur, and the macro-petrographic type is semi-dural to semi-lariferous coal with high maturity. The maximum vitrinite reflectance of the No. 3 coal seam in the research area is 1.4–2.4%, belonging to medium and high metamorphic coking coal-anthracite, with a large coal rank span (Figure 5). With the Lizhuang–Ximangou line as the boundary, it is obviously divided into north and south zones. The northern zone is relatively simple, and the contour line extends in the ENE direction. The vitrinite reflectance gradually increases from the NW orientation to the SE orientation, from 1.4% to 1.9%. The southern zone is characterized by two high-value centers in the east and south and a low-value center. The eastern center is EW-trending in the A502 and A904 areas, and the maximum vitrinite reflectance can reach 2.4%. The southern center is distributed in the area of L1505 and extends in the NEN orientation, and the maximum vitrinite reflectance reaches 2.5%. The relatively low-value center is clamped and distributed in the NW orientation, and the maximum vitrinite reflectance is as low as 1.9%. It can be seen that the maturity of the South Anze No. 3 coal seam is high, the maximum vitrinite reflectance is mostly higher than 1.9%, and the coal rank reaches a high metamorphic grade lean coal to anthracite, especially in the south of the study area where the maximum vitrinite reflectance is above 1.9%. It shows that the South Anze No. 3 coal seam has reached maturity to over maturity, and a good coalbed-methane reservoir can be formed if there are good preservation conditions in geological history.

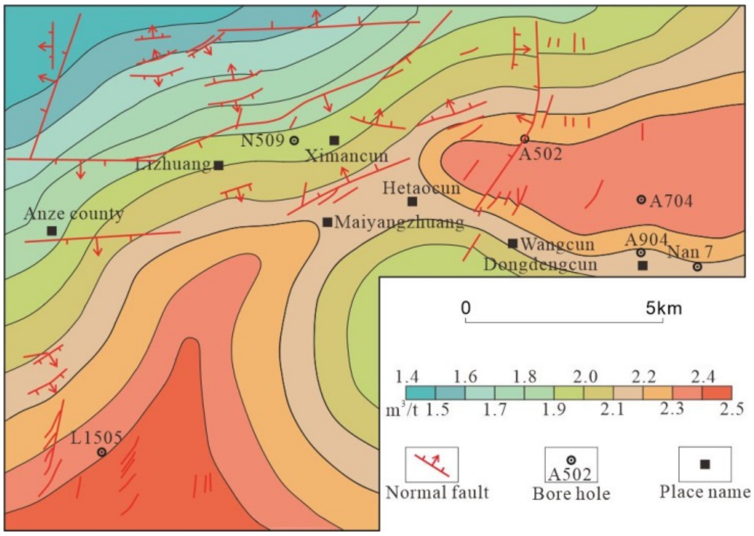

Figure 5. The maximum vitrinite reflectance contour map of the No. 3 coal seam in South Anze.

(ii) The reservoir of the No. 3 coal seam

The overall coal texture of the South Anze No. 3 coal seam is intact, the fracture is not developed. However, the stress concentration part of local structural development (two wings of an anticline with strong deformation), there is strong deformed coal developed, which is in powder form. Regarding the permeability of the No. 3 coal seam, referring to the adjacent Anze block, the permeability of raw coal is generally less than 5×10^{-7} μm^2, far lower than the lower limit of permeability of an effective coal reservoir in China devised by Kang et al. (2017) [35], which is consistent with the characteristics of undeveloped fractures in the study area. Liu et al. (2010) [36] calculated the gas saturation in the Anze block to be 5.70–88.33% based on the relationship between vitrinite reflectance and Langmuir volume and pressure, and in combination with isothermal adsorption equation, which can be used as the reference for the gas saturation in the study area.

3.3. Preservation Conditions of the No. 3 Coal Seam

Groundwater systems and roof lithology are two main factors which determine the preservation conditions of coalbed methane. The groundwater system in the study area includes four independent aquifers [7,37], which are the karst fissure aquifer of the Ordovician Fengfeng formation and the Taiyuan formation of the late Carboniferous–early Permian, the fissure clastic rock aquifer of the Shanxi formation, and the unconsolidated pore aquifer of the Quaternary, in which the aquifer of the Shanxi formation is mainly K7 and K8 aquifers located above and below the No. 3 coal seam, respectively, and has a hydraulic connection with the No. 3 coal seam, but the water quantity is low.

The sedimentary period of the Shanxi formation in the study area was dominated by an inter-distributary bay in the delta front [38]. The No. 3 coal seam roof, mainly composed of mudstone, sandy mudstone, and argillaceous sandstone sandwiched with banded sandstone, was formed (Figure 6). Different lithologies are distributed in an NEN-oriented strip-like pattern, and are mainly controlled by two distributary channels located in the east of Anze and the north of Wangcun, respectively. The channel is a sandstone deposit, and argillaceous sandstone, sandy mudstone, and mudstone are symmetrically developed on both sides. The NEN-oriented mudstone belt across Maiyangzhuang is distributed between two channels, and the mudstone developed in Wangcun is the product of the southward secondary branch channel of the right channel in the study area. In general, in terms of lithologic combination, the shale content of the roof strata in the study area is high, which is conducive to coalbed-methane storage from the perspective of lithology.

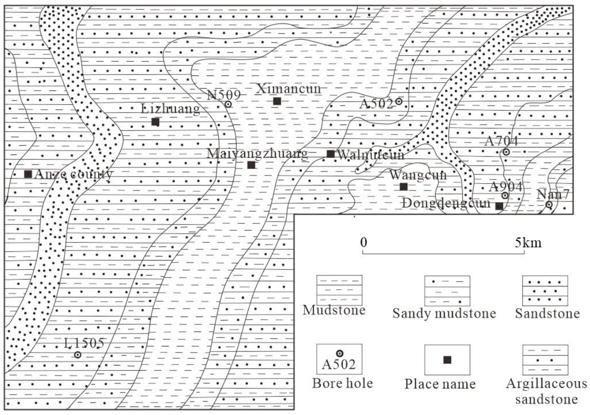

Figure 6. Roof lithology distribution map of the No. 3 coal seam in South Anze.

4. Structural Characteristics and Genesis

Using the method of structural analysis, the South Anze structural deformation field and structural division were determined, based on the structural-type analysis. The formation mechanism is discussed by combining the regional and geotectonic backgrounds. In order to better analyze the fold assemblage characteristics, this study extended the scope of the No. 3 coal seam floor structure map to the south by including data from four boreholes (zk105, zk501, zk505, and zk509) outside the study area (Figure 7).

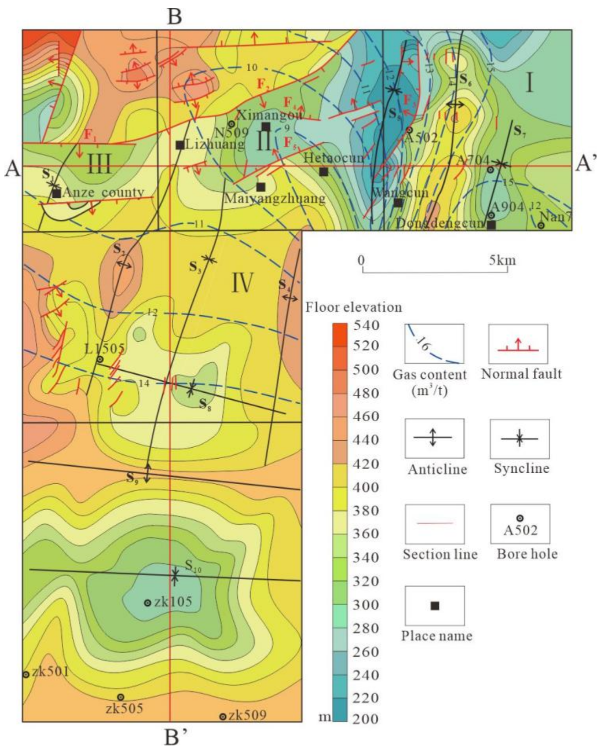

Figure 7. Structural zoning and gas content contour map of the South Anze No. 3 coal seam.

4.1. Structural Type

The types of structure in the South Anze area can be divided into two major categories: fold and fault. The faults can be subdivided into normal faults and strike-slip faults.

(i) Fold

In general, the study area is located on the west wing of the wide and gentle Qinshui Syncline. Therefore, the secondary folds in the study area are weakly deformed, and the syncline is wide, the anticline is relatively closed, which is similar to the ejective folds, but because of their weak deformation, they are different from the ejective folds, so they are called ejective-like folds. The folds are divided into two categories depending on the direction of the fold axis: EW-trend "ejective fold" and NEN-trend "ejective fold".

EW-trend "ejective folds" are mainly located in the southern part of the study area. For example, the S_8 syncline, which is located near well L1505, has a WNW-oriented axis, with both wings wide, and the S_9 anticline, which is located to the south of the S8 syncline has a near EW-oriented axis, with both wings tightly closed.

NEN-trend "ejective folds" are superimposed on the EW-trend folds, and distributed throughout the region, but more developed in the northern part. For example, the S_7 syncline, which is located east of well A704, has an NEN-oriented axis and the two wide and gentle wings superimpose on the EW-trend folds. The S_6 anticline, which is located on the west side of the S_7 syncline, has short extensions on both wings and forms an "ejective fold" together with the S_7 syncline.

(ii) Normal fault

The normal fault is widely developed in the study area and mainly located in the north. According to its trend, it can be roughly divided into four types: NEN-trend normal fault, ENE-trend normal fault, WNW-trend normal fault, and near EW-trend normal fault.

The NEN-trend normal fault is mainly located in the eastern part of the study area, with sporadic development in the northwest. The trend is roughly parallel to the NEN-trend "ejective fold" above. For example, the F_3 fault, under its control, forms a fault depression on the west side of the fault.

The ENE-trend normal fault is mainly located in the central part of the study area. For example, the F_2 fault, which extends farther and plays a controlling role in the depth of the northern part of the study area.

The WNW-trend normal fault is rare, and sporadically developed in the middle of the study area, interspersed between ENE-trend normal faults. For example, see the F_4 fault.

The EW-trend normal fault is mainly located in the western part of the study area. For example, the F_1 fault, which cuts the ENE-trend fault to the east, controls the depth of burial in the northwestern part of the study area together with it.

(iii) Strike-slip fault

The strike-slip faults in the study area are rare, small in scale, NEN-trending, and concentrated to form two groups of echelon assemblage in the southwest of the study area.

4.2. Structural Deformation Field and Partition

The structural deformation field can be classified into three types: compression, extension, and shear. The compressive deformation field is most developed and subdivided into NS and WNW–ESE according to the compressive direction. The former is more developed towards the south, while the latter is more developed towards the east (Figures 7–9). Comparing the three types of deformation, compression, and shear deformation formed earlier, while extensional deformation mainly showed the superposition on the fault formed in the previous deformation process, so the faults in the area are mainly normal fault. Further, in combination with the distribution of different deformation fields, South Anze is divided into four structural divisions (Figure 7):

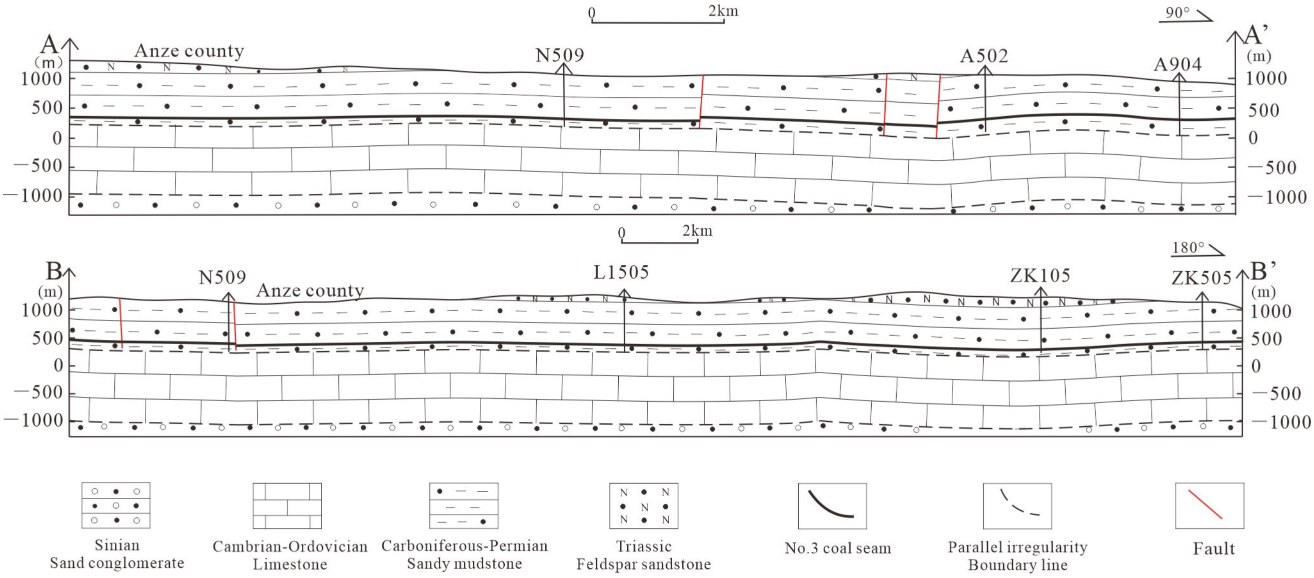

Figure 8. Geological sections in the South Anze area.

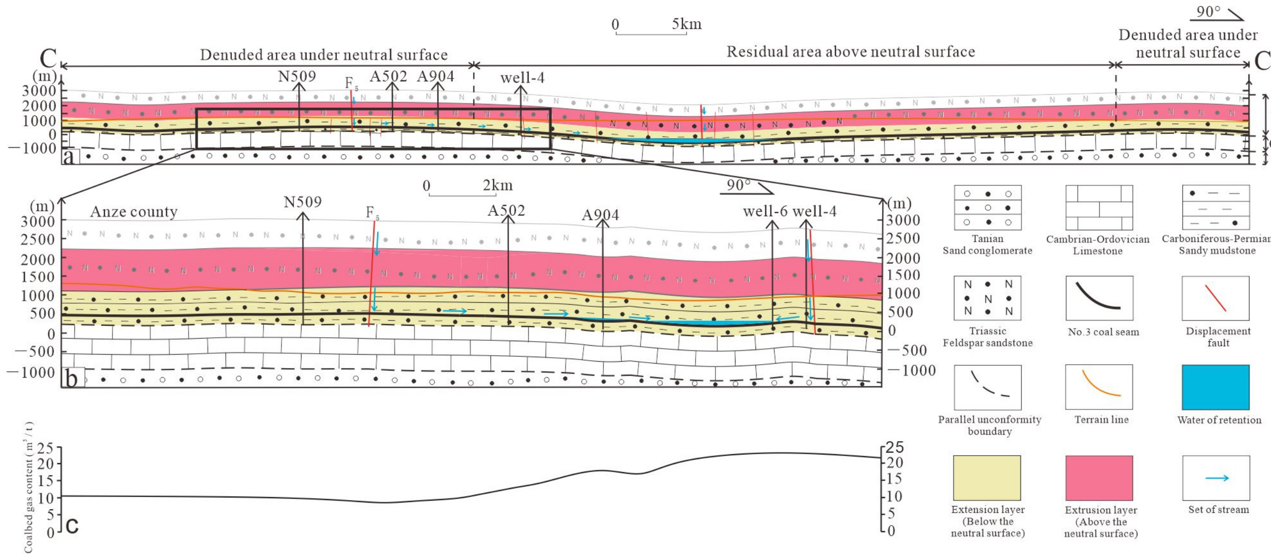

Figure 9. Geological model and coalbed-methane accumulation model of CC′ in the southern Qinshui Basin [7,39]. (**a**) Geological model and coalbed-methane accumulation model of the southern Qinshui Basin. (**b**) Geological model and coalbed-methane accumulation model of the south Anze. (**c**) Coalbed-methane content curve of the south Anze.

(i) NEN compressive structural deformation area

Located in the east of the study area (Area I in Figure 7), this area is mainly characterized by the development of NEN-trending gentle folds and normal faults. According to the elevation contour line of the No. 3 coal seam floor, three continuously developed folds can be delineated from west to east, and the two wings of the synclines are wider compared to the middle anticline, indicating different equal development of the folds. The deformations are both weak as shown in profile AA′ (Figure 8). At the same time, the contour lines of the fold core (especially the anticline in the middle) are shown as alternating oval shapes, reflecting the characteristics of a mainly NEN-trend "ejective fold" in this deformation zone, superimposed with a near EW-trend fold. As for the development of normal faults, it is due to the structural inversion caused by superimposed extensional deformation, and their formation should initially be a reverse fault.

(ii) ENE shear fracture deformation area

Located in the north–central part of the study area (Area II in Figure 7), this area is mainly developed with ENE normal faults, with partial EW and WNW normal faults. The ENE-trending normal fault is oblique to the WNW–ESE compressional stress direction with an angle less than 45°, which indicates that the ENE-trending normal fault was originally a group of conjugate shear faults developed under the compressional stress in this direction, and then reversed to form a normal fault due to the superimposition of extensional deformation. The WNW-trending normal fault is a normal fault formed along the direction of compressive stress under the action of simultaneous compression. The EW normal fault should be the result of near SN-oriented compressional deformation superimposed on the later extension deformation. Controlled by fault inversion, especially the large-scale N509 north normal fault and the A502 normal fault in Zone I, the area sandwiched by the two faults in Zone II constitutes the low-value area of the floor elevation of the No. 3 coal seam in the study area. The overall elevation value decreases to the north and east (near the fault direction) and gradually increases to the south.

(iii) EW compressive fracture deformation zone

Located in the northwest of the study area (Area III in Figure 7), this area is mainly developed with near EW-trend faults, and locally present with near NS-trend and NEN-trend faults. The near EW-trending fault should initially be a reverse fault formed under the near NS-oriented compressive stress, and later superimposed extensional deformation inversion to form a normal fault. The near NS-trend fault is formed along simultaneous compressive stress. The NEN-trend fault is limited by the EW-trend fault, indicating that it is formed late, so it should be the result of WNW–ESE compressive stress superimposed extension deformation. The contour of the elevation of the No. 3 coal seam floor around the fault generally extends in the NEN-orientation, and the elevation decreases from the periphery to the center, indicating a NEN-trend syncline, which is also a response to WNW–ESE compression.

(iv) EW-oriented compressive fold deformation area

Located in the south of the study area (Area IV in Figure 7) and its southern extension area, this area is mainly developed with near EW-trend gentle folds, superimposed with NEN folds, and locally seen with ENE normal faults and left-step echelon faults with the echelon axis extending in the NS direction. Three continuously developed folds can be delineated from north to south, and the syncline on both sides is wider than the anticline in the middle, which also presents a "ejective fold" assemblage (Figure 8). At the same time, the contour line along the fold axis also shows an oval shape arranged alternately, reflecting that the folds in this deformation zone are dominated by an EW-trending "ejective fold" assemblage and superimposed with NEN folds. As for ENE-trending normal faults, the genesis is the same as that of the same direction faults in Area II, while the echelon faults are related to the near-NS-trend dextral shear stress generated by the dextral slip between the Ordos block and the Shanxi block in the region caused by the tectonic movement of the Neo-Tethys tectonic domain in the Cenozoic era.

In general, South Anze is an eastward-plunging nosing structure, which is superimposed by secondary folds and faults, further complicating the coal seam occurrence. NEN-trending and EW-trending "ejective fold" assemblages are formed in the east and south, respectively, and NEN-trending normal fault assemblages and controlled fault depression areas are formed in the middle.

4.3. Structure-Formation Mechanism

Based on the regional tectonic evolution background and the deformation field and its distribution characteristics in South Anze, the formation of NEN-trending compressive structures and ENE-trending normal faults (shear faults in the early stage) in the study area is attributed to the WNW–ESE compressive stress in the early Yanshanian. The formation of NS-trending echelon faults and many structural inversion normal faults is attributed to the long-term extensional background since the late Yanshanian and the simple shear stress field caused by the NS-trending right-lateral strike-slip of the Ordos and Shanxi blocks caused by the orogeny of the Neo-Tethys tectonic domain since the Cenozoic. As for the near EW-trend compressional structures, it may be the NS-trending compression of THE Hercynian or Indosinian. Considering that the development degree of the compressive structure in this direction weakens from south to north and the latest strata involved in the structure are Triassic, the former indicates that the source direction of the force is from the south, and gradually weakens in the process of northward transmission, and the degree of structural development weakens. The latter limits the deformation time to be after the Triassic, and the two phases confirm that the nearly EW-trending compressive structure is formed in the south–north compressive tectonic stress field caused by the orogeny of the Paleo-Tethys tectonic domain in the Indosinian period. Therefore, the formation process of the structure in the study area is described as follows:

(i) Indosinian

In the Triassic, the North China Plate completely collated with the South China Plate, resulting in compression stress in approximately an SN direction [40]. Although the study area is located in the hinterland of the North China plate, the stress action can still be transferred to this area, and a gentle anticline (the predecessor of the nosing and low uplift structure) extending in the EW direction and plunging eastward is formed in the region. South Anze formed a secondary "ejective fold" assemblage with gradually weak deformation from south to north, a zone III EW reverse fault, and a near NS-trend fault, which was superimposed on the anticline.

(ii) Early Yanshanian

In the middle-late Jurassic, the North China plate was mainly affected by the subduction of the Pacific plate under the background of plate convergence [33,41], which is a strong compression intracontinental orogenic period [42,43]. The WNW–ESE compressive tectonic stress field is formed, which formed the NEN-trending Qinshui Syncline and superimposed upon the early EW-trending anticline. The nosing structure is formed in the west wing of the Qinshui Syncline, and the low uplift is formed at the hinge. In South Anze, the NEN-trending secondary "ejective fold" assemblage weakened from east to west is also superimposed on the previously formed near EW-trend "ejective fold" assemblage, as well as the NEN-trend compressive reverse faults in Areas I and III and the NEN-trending shear faults in Area II.

(iii) Late Yanshanian–Himalayan

The early Yanshanian compressional uplift and orogenic movement resulted in the great crustal thickening of the North China Block, thus inducing the lithospheric collapse and thinning and craton destruction centered on North China [33]. The North China region including the study area entered the post-orogenic stress relaxation and extension stage during the late Yanshanian.

During the Himalayan period, the study area was affected by the combined effects of the subduction and retreat of the Pacific plate and the collision of the India-Eurasia plate. While continuing the general extensional background, the Shanxi block was up-lifted widely and the Ordos block rotated counterclockwise due to the long-range effect of the rapid uplift of the Qinghai-Tibet Plateau. The rotation rate of the Shanxi block is smaller than that of the Ordos block, forming a near NS-oriented dextral couple, which should be the cause of the formation of the echelon faults in Area IV. The long-term extension background since the late Yanshanian has caused the structural development characteristics of normal faults in the area. At the same time, the NW–SE tensile stress derived from the NS-trending right-lateral couple increases the ENE-trending fault offset, making Area II dominated by ENE-trending faults in the nosing-uplift area become a relatively subsag unit in the South Anze area.

5. Gas Accumulation under Control of Tectonism

First, we analyze the control of the South Anze structure on coalbed-methane accumulation and verify the law of gas enrichment in syncline in the Qinshui Basin. We also embed the process of coalbed-methane generation and migration in the geological process of coal measure deformation and denudation after coal formation. Finally, we discuss the genetic mechanism of syncline gas enrichment and construct a model to represent it.

5.1. Control Law of South Anze Structure on Coalbed Methane

After analyzing the various factors affecting the enrichment of No. 3 coalbed methane in the South Anze area, it was found that coal quality and high coalification are favorable for gas generation. Additionally, weak deformation and hydrodynamic conditions, large and stable thickness, moderate burial depth, and an argillaceous rock-dominated roof are also favorable for coalbed-methane enrichment. As a result, the coalbed-methane content in the study area is relatively high, reaching 9–15 m^3/t. However, the gas content varies across the plane and is strongly related to the structural division (as shown in Figure 7).

Areas I and IV, which are characterized by an "ejective fold", are high-value areas for coalbed-methane content. Conversely, Area II, which is characterized by ENE trending normal faults, is the low-value area. Zone III, dominated by EW-trend normal faults, has medium coalbed-methane content. It is not difficult to understand the low content of coalbed methane in the central ENE–oriented fault development area. The ENE-trending faults in the study area are concentrated in the central part, and the faults in this direction are most conducive to opening under the NW–SE extension stress induced by the Cenozoic near NS-oriented shearing and easily release coalbed methane. Therefore, it has become a low-value area in South Anze. In addition, an area with low coalbed-methane content is also developed in the east of Dongdeng Village in the study area. Compared with the contour map of the coalbed-methane content of the No. 3 coalbed in Mabi in the adjacent area, there is also an area with low coalbed-methane content in the southeast of Dongdeng Village [44]. However, due to the lack of available materials for analysis, this cannot be reasonably explained.

On the other hand, there are high-value areas in the east and south, with structural characteristics that are similar. Both areas are characterized by an "ejective fold" developed on gentle slopes. The eastern part is developed on a gentle slope controlled by a nosing structure that gradually rises from east to west, and the southern part is developed on a gentle slope from north to south controlled by nosing uplift and fault depression. These findings further confirm the understanding of syncline gas accumulation in the Qinshui Basin.

5.2. Syncline Accumulation Model in Qinshui Basin

(i) The proposal of conceptual model

Previous literature has mentioned the syncline reservoir formation in Qinshui Basin, which can be divided into two scales. Firstly, the coalbed-methane content increases gradually from the basin margin to the basin across the whole Qinshui Basin [38]. Secondly, it is the secondary fold in the basin, and the coalbed-methane content is higher in the tectonic trough area of the small-scale syncline [10]. In addition to this area, this pattern has also been found in blocks such as Fanzhuang, Panzhuang, and Anze [7,32,45]. As for the origin, some scholars believe that tensile stress is developed in the coal seam and its roof around the anticline axis from the perspective of structure, which is beneficial to the dissipation of coalbed methane, while the core of syncline and adjacent areas have a higher reservoir pressure, which is beneficial to the preservation of coalbed methane [9,31]. Other scholars emphasize the coordination of structural and hydrodynamic conditions and point out that the sealing effect of hydrostatic pressure is the key to the reservoir formation at the structural low point with detained water [7,10].

Our understanding of syncline reservoir formation has been significantly improved based on previous studies on the reservoir-forming mechanism of the Qinshui Basin, but it is still in the initial stage, and some key processes in the reservoir forming process have not been considered, such as where the neutral surface is located. Additionally, some key phenomena have not been reasonably explained, such as the low gas saturation in the Qinshui Basin. In this study, we aim to restore the basin structure after Yanshanian deformation and discuss the syncline reservoir-forming mechanism of the Qinshui Basin using the CC′ section in the south of the Qinshui Basin as an example (Figure 1).

After the formation of the late Paleozoic coal measures in the Qinshui Basin, the basin experienced three tectonic cycles of the Indosinian, Yanshanian, and Himalayan. Among them, the burial depth and coalification degree of the coal seam in the Indosinian continuously increased, and the contribution to the current coalbed-methane content was small due to the small amount of hydrocarbon generation and the uplift at the end [7]. In the early Yanshanian, only local areas received short-term sedimentation. In the end, it was affected by the extrusion of the eastern Kula Pacific plate, forming the main syncline of the Qinshui Basin and superimposing the secondary folds on it. Since then, it has been in a state of uplift and denudation [7]. The magma intrusion in the late Yanshanian greatly improved the coalification degree and led to the occurrence of a gas generation peak [46]. Whether the coalbed methane generated can be preserved or not in the following geological history is the main reason for determining the current coalbed-methane content. The fact that the gas saturation in the Qinshui Basin is not high and changes greatly also shows that the gas retention conditions in the basin are poor and change differently after the gas generation peak. Therefore, exploring the syncline reservoir formation in the study area requires a focus on the structure and tectonic stress state of coal measures and overlying strata in the Qinshui Basin caused by WNW–ESE compression in the early Yanshanian and the evolution process of the groundwater system in the subsequent denudation process.

(ii) Production of geological model

The geological model represents the stratigraphic texture and structural development state of the Qinshui Basin formed during the early Yanshanian movement (end of Middle Jurassic). The model will be based on the CC′ (Figure 1) section in the south of the Qinshui Basin and will be completed in three steps:

Firstly, the recovery of stratigraphic texture: Based on the regional stratigraphic summary (Table 1) and geological evolution process of the Qinshui Basin, the Middle Jurassic Heifeng formation is the latest stratum to receive deformation at the end of the Middle Jurassic. However, since the Middle Jurassic is only locally and sporadically developed, it is not considered during modeling.

Therefore, the latest strata that have undergone deformation should be the Upper Triassic Yanchang formation. However, considering the impact of the Indosinian movement, the overall uplift and erosion amount in the study area is about 500 m [46], so the top boundary of the strata that have undergone deformation should be about 500 m below the top surface of the Yanchang formation. In order to better demonstrate the stratigraphic texture of the basin, the oldest strata exposed in the area, the Sinian system, are used as the base of the model, thus forming the stratigraphic texture of the model, the stratigraphic texture contains two parallel unconformity surfaces, and three structural layers, namely, Z, Ꞓ-O, and C-T. The simplified stratigraphic section is drawn according to the thickness and main lithology of each structural layer (Figure 9a).

The second is the restoration of structure and stress state: including fold, fault, and stress state caused by longitudinal bending in coal measures. At the end of the Middle Jurassic, the study area experienced two stages of compressive stress, which are Indosinian NS compression and early Yanshanian WNW–ESE compression. The deformation during the Indosinian mainly showed the overall uplift of the entire Qinshui Basin, but for South Anze, a near EW-trend anticline was formed, and the Qinshui Syncline was superimposed later to form a nosing structure. The early Yanshanian compression was strong, and besides the formation of the Qinshui Syncline, there were also longitudinal reverse faults, transverse normal faults, and oblique strike-slip faults developed. Combined with the location of section CC′, the structure includes the whole Qinshui Syncline, the nosing structure of

South Anze, and the faults and secondary folds superimposed on it. As for folds and faults, they are drawn mainly according to the floor structure map of the No. 3 coal seam in Anze and South Anze, excluding the influence of Cenozoic tectonic inversion, and then extrapolated to the upper and lower horizons, but this only covers the west wing of Qinshui Syncline. As for the fluctuation of the east wing, it is based on the characteristics of the symmetrical development of both wings of the Qinshui Syncline [43], symmetrically plotted in conjunction with the geological map (Figure 9a). As the CC′ section is too large to reflect the secondary fold relief, the enlarged section of the west wing is drawn (Figure 9b).

The above is the drawing of the structure. For the stress state of the coal measures caused by the longitudinal bending of the Qinshui Syncline, it is necessary to consider the influence of the neutral plane. In terms of basin scale, the parallel unconformity interface can be used as the boundary, and the stressed stratum can be divided into three relatively independent single layers, corresponding to the above three structural layers. Here, we focus on the C-T structural layer containing the coal-bearing stratum. Considering that the Triassic system had been denuded for about 500 m when the Qinshui Syncline was formed, the neutral surface of the C-T structural layer should be located at the middle line of the structural layer after 500 m is subtracted from the top of the structural layer, and the green area above it is the compression area. The red area below is the extension area.

Finally, the topographic line, the No. 3 coal seam, and CBM content curve: The topographic line are drawn regarding the elevation read from the satellite map and in combination with the exposed geological boundary in the geological map. The No. 3 coal seam is characterized by thickening based on its floor elevation line. In order to discuss the corresponding relationship between fold development and coalbed-methane enrichment, the coalbed-methane content change curve (Figure 9c) through the section is drawn in combination with the isopleth of the coalbed-methane content of the No. 3 coal seam in Anze and South Anze.

(iii) Characteristics of geological model

Based on the consideration of coalbed-methane preservation, the characteristics of the model are summarized (Figure 9a) as the basis of the subsequent explanation of the reservoir formation mechanism:

Firstly, the No. 3 coal seam is located in the extensional stress area under the neutral plane of the C-T structural layer, close to the bottom of the structural layer, and the same applies to the K7 aquifer above it. This indicates that the extensional stress suffered by it is larger than that inside the structural layer. If there is no stagnant water plugging, the generated coalbed methane will diffuse upward to the neutral plane and be plugged by the overlying compressive stress area. This way, it can be temporarily stored in the reservoir between the coal seam and the neutral plane.

Secondly, according to the intersection relationship between the neutral plane and the ground, the section can be divided into three parts on the left, middle, and right. The neutral plane of the left and right parts is almost coincident with the ground. The compressive stress area above the neutral plane is completely eroded, and the temporarily stored coalbed methane under the neutral plane is lost. This further leads to the loss of coalbed methane in the coal seam. In the middle part, there is still a compressive stress zone above the neutral plane. The closer to the syncline center, the greater the thickness, and the better the preservation of the underlying coalbed methane.

Thirdly, South Anze is controlled by an EW anticline, so the NS extensional stress environment is superimposed above the neutral plane, which makes it more suitable for coalbed methane to dissipate.

Fourthly, among the faults formed by the early Yanshanian movement, the transverse normal faults are not developed, the longitudinal reverse faults are closed and do not conduct water and gas, and the oblique strike-slip faults can become an important water and gas channel, which affects the formation of coalbed-methane reservoirs.

(iv) Description of the reservoir formation mechanism

The geological model above indicates that during the formation of the Qinshui Syncline at the end of the Middle Jurassic, the No. 3 coal seam was in an extensional stress environment that was unfavorable for coalbed-methane aggregation. The upward diffusion path of coalbed methane can only be blocked if water is stored in the K7 aquifer. The earlier the water is stored, the less it dissipates, and the more it enriches. However, it should be asked: where does the water come from? Currently, the groundwater recharge area at the basin edge is only exposed to the surface. How do atmospheric precipitation and surface water recharge the K7 aquifer? Based on the geological model, two possible supply channels are speculated:

Firstly, the extensional stress zone below the neutral plane of the anticline formed during the Indosinian and early Yanshanian, For example, the EW-trend nosing structure and the secondary anticlines of "ejective fold" formed. The extensional stress zone of such structures can make the pores and fissures in the strata communicate and allow surface water to permeate downward. Although the deformation of the study area is weak, and the pore communication is not strong, it can still be used as a supply channel under the large time scale of geological history with the unit of million years. The channel is coordinated with the extensional stress area under the neutral plane of the Qinshui Syncline and completes the supply of surface water to the K7 aquifer.

Secondly, the faults formed by the early Yanshanian movement have been mentioned above. Among the three types of faults, longitudinal reverse faults and transverse normal faults have little influence, and oblique strike-slip faults can be used as good channels to connect the surface with the K7 aquifer. For example, the F_5 fault, which is located in the north of Maiyangzhuang, is a normal fault trending towards the ENE. It is located in the ENE-trending shear fault deformation zone; thus, its strike is oblique to the extrusion stress direction of the ESE–WNW in the early Yanshanian, indicating that this fault was formed as a conjugate shear translational fault at the beginning, and later superimposed extensional deformation and then became normal faults, which facilitate the conduction of groundwater. According to Figure 9b, this fault runs through the K7 aquifer and the surface and is one of the sources of stagnant water.

After the K7 aquifer receives recharge, it can flow from the two wings of the Qinshui Syncline to the core. The seepage from the wing to the core should be very slow due to the slow recharge process and the low water volume of the K7 aquifer. Moreover, due to the development of secondary anticlines, especially the anticlines of "ejective fold", the secondary synclines can also store water, while the secondary syncline at the core of Qinshui Syncline is more conducive to water storage. In this process, the syncline core can receive the supply from both wings in addition to the channel supply from the overlying strata, so the water storage is faster and the syncline reservoir in the Qinshui Basin is formed. Moreover, the strata in the compressive stress area above the neutral plane of the core provides an additional layer of protection, resulting in a higher coalbed-methane content (Figure 9b,c).

6. Conclusions

This paper provides a structural analysis of the No. 3 coal seam floor in the South Anze area, identifying factors that influence coalbed-methane enrichment. The study examines the control of structure on coalbed-methane enrichment and the geological evolution process of the area. The gas enrichment reservoir forming mode of the syncline in the Qinshui Basin is also discussed. It provides ideas and references for the study of coalbed-methane accumulation in weakly deformed syncline basins around the world. The key findings are as follows:

(i) The floor structure of the South Anze No. 3 coal seam was mainly formed by the compressive stress deformation fields in the WNW–ESE and NS directions and was reformed by the extensional stress field in the later period. The whole structure is a nosing structure plunging from west to east with superimposed secondary folds and faults in different directions. Four deformation zones can be divided, i.e., NEN-trending compressional structure, NEN-trending shear fault, EW-trending compressional fault, and EW-trending compressional fold. Indosinian and Yanshanian compression and Himalayan fault inversion are the key factors to form the tectonic assemblage in the study area.

(ii) Tectonic action is the key factor in coalbed-methane accumulation in the No. 3 coal seam in the study area, and folding is the main controlling factor of coalbed-methane accumulation. The ENE-trending shear fault deformation area located in the nosing uplift became a low coalbed-methane content area due to gas dispersion during the Himalayan extension. The syncline in the NEN and EW-trending "ejective fold" combination in the west and south of the study area is the high-value area of coalbed-methane content. It is further verified that the law of syncline gas accumulation in the Qinshui Basin is also applicable to the wing of the Qinshui Syncline.

(iii) The stagnant water formed during the geological history is the key factor of gas enrichment in the syncline of the Qinshui Basin. Since the formation of the Qinshui Syncline, the main coal seam has been in an extensional environment below the neutral plane, resulting in the main dissipation of coalbed methane. During its geological history, surface water penetrated into the aquifer above the main coal seam through two channels: the extensional area above the neutral plane of the adjacent anticline and the shear fracture. A hydrostatic pressure seal is formed in the Qinshui Syncline and its superimposed secondary syncline, which provides good structural and hydrological conditions for gas enrichment in the Qinshui Basin syncline.

Author Contributions: Methodology, Z.Q.; investigation, Z.Q.; resources, B.W.; data curation, B.W.; writing—original draft, Q.Z.; writing—review & editing, B.W. and Z.Q.; visualization, Q.Z.; supervision, B.W. and Y.Z.; project administration, Y.Z. All authors have read and agreed to the published version of the manuscript.

Funding: This work was supported by the Jiangsu Province Carbon Peak Carbon Neutral Technology Innovation Project in China (Grant No. BE2022034) and the Research and Application of Key Technologies for High Gas, Three Soft, Extra Thick, and Low Permeability Coal Seam Vertical Collaborative Precision Extraction.

Data Availability Statement: The data source has been explained in the text.

Acknowledgments: We thank the reviewers for their valuable comments and the help provided by Li Changxing and Zhao Hongzhong in drawing.

Conflicts of Interest: The authors declare no conflict of interest.

References

1. Creedy, D.P. Geological controls on the formation and distribution of gas in British coal measure strata. *Int. J. Coal Geol.* **1988**, *10*, 1–31. [CrossRef]
2. Song, Y.; Zhao, M.; Liu, S.; Wang, H.; Chen, Z. Influence of Tectonic Evolution on the Degree of Coalbed Methane Enrichment. *Chin. Sci. Bull.* **2005**, *50*, 1–5. [CrossRef]
3. Liu, H.; Li, J.; Wang, H.; Zhao, Q. Different effects of hydrodynamic conditions on coal BED gas accumulation. *Nat. Gas Ind.* **2006**, *26*, 35–37. [CrossRef]
4. Qin, Y.; Jiang, B.; Wang, J.; Wu, C.; Fu, X.; Wei, C.; Hou, Q.; Ju, Y. Coupling Control of Tectonic Dynamical Conditions to Coalbed Methane Reservoir Formation in the Qinshui Basin, Shanxi, China. *Acta Geol. Sin.* **2008**, *82*, 1355–1362. [CrossRef]
5. He, L. Tectonic and Structural Controls on Gas Accumulation Characteristics in the Weibei Coalbed Methane Pilot-Production District. Master's Thesis, China University of Geosciences (Beijing), Beijing, China, 2012.
6. Yao, Y.; Liu, D.; Yan, T. Geological and hydrogeological controls on the accumulation of coalbed methane in the Weibei field, southeastern Ordos Basin. *Int. J. Coal Geol.* **2014**, *121*, 148–159. [CrossRef]
7. Chen, S.; Tao, S.; Tian, W.; Tang, D.; Zhang, B.; Liu, P. Hydrogeological control on the accumulation and production of coalbed methane in the Anze Block, southern Qinshui Basin, China. *J. Pet. Sci. Eng.* **2020**, *198*, 108138. [CrossRef]
8. Geng, M.; Chen, H.; Chen, Z.; Li, G.; Deng, Z.; Li, Y. New recognization of CBM enrichment pattern and resource potential in China. *Nat. Gas Geosci.* **2016**, *27*, 1659–1665. [CrossRef]
9. Liu, D.; Jia, Q.; Cai, Y.; Gao, C.; Qiu, F.; Zhao, Z.; Chen, S. A new insight into coalbed methane occurrence and accumulation in the Qinshui Basin, China. *Gondwana Res.* **2022**, *111*, 280–297. [CrossRef]

10. Liu, D.; Yao, Y.; Wang, H. Structural compartmentalization and its relationships with gas accumulation and gas production in the Zhengzhuang Field, southern Qinshui Basin. *Int. J. Coal Geol.* **2022**, *259*, 40–55. [CrossRef]
11. Li, G.; Wang, H.; Wu, L.; Liu, H. Theory of syncline conteolled Coalbed methane. *Nat. Gas Ind.* **2005**, *25*, 26–28. [CrossRef]
12. Qian, K.; Zhao, Q. *Exploration and Development Theory and Experimental Testing Technology of Coalbed Methane Gas*; Petroleum Industry Press: Beijing, China, 1996.
13. Sang, S.; Fan, B.; Qin, Y.; Tang, S.; Ye, J.; Jia, S. Conditions of Sealing and Accumulation in Coal Bed Gas. *Oil Gas Geol.* **1999**, *20*, 8–11.
14. Sang, S.; Han, S.; Liu, S.; Zhou, X.; Li, M.; Hu, Q.; Zhang, C. Comprehensive study on the enrichment mechanism of coalbed methane in high rank coal reservoirs. *J. China Coal Soc.* **2022**, *47*, 388–403.
15. Zhang, Y.; Yan, J.; Wang, W. Study on the types of coalbed gas deposits based on the fold neutral plane. *J. Saf. Environ.* **2015**, *15*, 153–157. [CrossRef]
16. Tang, Y.; Gu, F.; Wu, X.; Ye, H.; Yu, Y.; Zhong, M. Coalbed methane accumulation conditions and enrichment models of Walloon Coal measure in the Surat Basin, Australia. *Nat. Gas Ind. B* **2018**, *5*, 235–244. [CrossRef]
17. Xin, F.; Xu, H.; Tang, D.; Cao, C. Differences in accumulation patterns of low-rank coalbed methane in China under the control of the first coalification jump. *Fuel* **2022**, *324*, 46–57. [CrossRef]
18. Finch, W.I.; Huffman, A.C.; Fassett, J.E. *Coal, Uranium, and Oil and Gas in Mesozoic Rocks of the San Juan Basin: Anatomy of a Giant Energy-Rich Basin: Sandia Mountains to Mesita, New Mexico June 30–July 7, 1989*; Wiley: Hoboken, NJ, USA, 2013. [CrossRef]
19. Hobbs, K.M.; Fawcett, P.J. A physical and chemical sedimentary record of Laramide tectonic shifts in the Cretaceous-Paleogene San Juan Basin, New Mexico, USA. *Geosphere* **2021**, *17*, 854–875. [CrossRef]
20. Baltz, E.H. *Stratigraphy and Regional Tectonic Implications of Part of Upper Cretaceous and Tertiary Rocks, East-Central San Juan Basin, New Mexico*; U.S. Government Publishing Office: Washington, DC, USA, 1967. [CrossRef]
21. Wainman, C.C.; Mccabe, P.J.; Crowley, J.L.; Nicoll, R.S. U–Pb zircon age of the Walloon Coal Measures in the Surat Basin, southeast Queensland: Implications for paleogeography and basin subsidence. *Aust. J. Earth Sci.* **2015**, *62*, 807–816. [CrossRef]
22. Scott, S.G. *The Geology, Stratigraphy and Coal Seam Gas Characteristics of the Walloon Subgroup-Northeastern Surat Basin*; James Cook University: Douglas, Australia, 2008.
23. Hamilton, S.K.; Esterle, J.S.; Sliwa, R. Stratigraphic and depositional framework of the Walloon Subgroup, eastern Surat Basin, Queensland. *Aust. J. Earth Sci.* **2014**, *61*, 1061–1080. [CrossRef]
24. Ayers, W.B.; Ambrose, W.A.; Kaiser, W.R.; Laubach, S.E.; Scott, A.R.; Yeh, J.S.; Tremain, C.M.; Whitehead, N.H., III. Geologic and hydrologic characterization of coalbed methane reservoirs, Fruitland Formation, San Juan basin, Colorado and New Mexico. In Proceedings of the Conference: Annual Meeting of the American Association of Petroleum Geologists (AAPG), Dallas, TX, USA, 7–10 April 1991. [CrossRef]
25. Ju, Y.; Qiao, P.; Wei, M.; Li, X.; Xu, F.; Feng, G.; Li, Y.; Wu, C.; Cao, Y.; Li, G. Typical patterns of coalbed methane enrichment and high yield under regional tectonic and evolutionary control. *Coalf. Geol. Explor.* **2022**, *50*, 1–12.
26. Jin, Z.; Wang, C.; Zhang, X. Deposition conditions of high quality reservoir development of Permi-Carboniferous coal in Qinshui Basin. *Acta Geol. Sin.* **2005**, *50* (Suppl. 1), 32–37.
27. Zhao, X.; Yang, Y.; Sun, F.; Wang, B.; Zuo, Y.; Li, M.; Shen, J.; Mu, F. Enrichment mechanism and exploration and development technologies of high coal rank coalbed methane in south Qinshui Basin, Shanxi Province. *Pet. Explor. Dev.* **2016**, *43*, 332–339. [CrossRef]
28. Li, M.; Liu, Q.; Zhang, J.; Wang, L. Relationship between structural style and CBM well productivity: A case study of the Jincheng coalfield. *Nat. Gas Ind.* **2010**, *30*, 10–13. [CrossRef]
29. Zhao, S.; Zhu, Y.; Cao, X.; Wang, H.; Zhou, Y. Control Mechanism and Law of Geological Structure Affected to Production Capacity of Coal Bed Methane Well. *Coal Sci. Technol.* **2012**, *40*, 108–111+116.
30. Liu, H.; Sang, S.; Wang, G.G.; Li, M.; Xu, H.; Liu, S.; Li, J.; Ren, B.; Zhao, Z.; Xie, Y. Block scale investigation on gas content of coalbed methane reservoirs in southern Qinshui basin with statistical model and visual map. *J. Pet. Sci. Eng.* **2014**, *114*, 1–14. [CrossRef]
31. Cai, Y.; Liu, D.; Yao, Y.; Li, J.; Qiu, Y. Geological controls on prediction of coalbed methane of No. 3 coal seam in Southern Qinshui Basin, North China. *Int. J. Coal Geol.* **2011**, *88*, 101–112. [CrossRef]
32. Su, X.; Lin, X.; Liu, S.; Zhao, M.; Song, Y. Geology of coalbed methane reservoirs in the Southeast Qinshui Basin of China. *Int. J. Coal Geol.* **2005**, *62*, 197–210. [CrossRef]
33. Dong, S.; Zhang, Y.; Long, C.; Yang, Z.; Ji, Q.; Wang, T.; Hu, J.; Chen, X. Jurassic Tectonic Revolution in China and New Interpretation of the Yanshan Movement. *Acta Geol. Sin.* **2007**, *81*, 1449–1461.
34. Meng, Y.; Wang, X.; Chen, J. Geological evidence of the Cenozoic tectonic uplift of the Taihang Mountains-Apatite fission track evidence from Well Qincan 1. *J. Guilin Univ. Technol.* **2015**, *35*, 15–28. [CrossRef]
35. Kang, Y.; Sun, L.; Zhang, B.; Gu, J.; Mao, D. Discussion on classification of coalbed reservoir permeability in China. *J. China Coal Soc.* **2017**, *42* (Suppl. S1), 186–194. [CrossRef]
36. Liu, Z.; Zhan, Q.; Wang, H. *Coalbed Methane Resource Prediction and Development Potential in Qinshui Coalfield, Shanxi Province*; 2010 National Coalbed Methane Symposium Papers; Sanyou Industrial Press: Beijing, China, 2010; pp. 184–191.
37. Wang, H.; Yao, Y.; Liu, D.; Pan, Z.; Yang, Y.; Cai, Y. Fault-sealing capability and its impact on coalbed methane distribution in the Zhengzhuang field, southern Qinshui Basin, North China. *J. Nat. Gas Sci. Eng.* **2015**, *28*, 613–625. [CrossRef]

38. Song, Y.; Ma, X.; Liu, S.; Jiang, L.; Hong, F.; Qin, Y. Accumulation conditions and key technologies for exploration and development of Qinshui coalbed methane field. *Pet. Res.* **2018**, *3*, 320–335. [CrossRef]
39. Meng, Z.; Lei, J.; Wang, Y. Evaluation of favorable areas for hydraulic fracturing of coal reservoir based on Griffith strength theory. *J. China Coal Soc.* **2020**, *45*, 268–275.
40. Wang, Y. Mesozoic-Cenozoic Structural Deformation and Tectonic Stress Field Characteristics in the Oinshui Basin. Ph.D. Thesis, Nanjing University, Nanjing, China, 2013.
41. Dong, S.; Zhang, Y.; Li, H.; Shi, W.; Xue, H.; Li, J.; Huang, S.; Wang, Y. The "Yanshan Movement" and the Late Mesozoic Multi Plate Convergence Structure of the East Asian Continent: Commemorating the 90th Anniversary of the "Yanshan Movement". *Chin. Sci. Earth Sci.* **2019**, *49*, 913–938.
42. Wang, T.; Yang, B. Source-rock Burial History of Triassic Yanchang Group Chang 7 Formation in Ordos Basin. *Liaoning Chem. Ind.* **2011**, *40*, 375–377. [CrossRef]
43. Liu, C.; Ge, X.; Qi, D. Burial history of Wangfu fault depression in Songliao Basin. *J. Heilongjiang Inst. Sci. Technol.* **2013**, *23*, 482–486. [CrossRef]
44. Liu, J. Coal Reservoir Modeling and the Optimization of Favorable Development Blocks in Anze Block of Qinshui Basin. Master's Thesis, China University of Geosciences (Beijing), Beijing, China, 2018.
45. Song, Y.; Liu, H.; Hong, F.; Qin, S.; Liu, S.; Li, G.; Zhao, M. Syncline reservoir pooling as a general model for coalbed methane (CBM) accumulations: Mechanisms and case studies. *J. Pet. Sci. Eng.* **2012**, *88–89*, 5–12. [CrossRef]
46. Zhong, Y.; Liu, D.; Yao, Y.; Cai, Y.; Hou, Y. Gas-bearing characteristics and tectonic control of coal reservoir in the Qinshui Basin of Anze area. *Earth Sci. Front.* **2017**, *24*, 342–352. [CrossRef]